

Target Image Video Search Based on Local Features

Bochen Guan, Hanrong Ye, *Student Member, IEEE*, Hong Liu, *Member, IEEE* and William Sethares, *Senior Member, IEEE*

Abstract—This paper presents a new search algorithm called Target Image Search based on Local Features (TISLF) which compares target images and video source images using local features. TISLF can be used to locate frames where target images occur in a video, and by computing and comparing the matching probability matrix, estimates the time of appearance, the duration, and the time of disappearance of the target image from the video stream. The algorithm is applicable to a variety of applications such as tracking the appearance and duration of advertisements in the broadcast of a sports event, searching and labelling painting in documentaries, and searching landmarks of different cities in videos. The algorithm is compared to a deep learning method and shows competitive performance in experiments.

Index Terms—Searching system, SIFT, Video searching

I. INTRODUCTION

Searching for target images in videos is a challenge in video processing and image processing [1–4]. Several approaches have been recently proposed [2–12] that show acceptable computational accuracy. Some [5–8] are well adapted to image-to-image searching but lack systematic estimation and modification for image-to-video searches. Others [2–4, 9–12], based on deep learning, require a large database for the training phase and such large data bases may be unavailable in many applications including the search for advertising images in a sports broadcast. Therefore, a target image searching system with high accuracy, fast search speed, significant robustness, and modest data requirements is needed for wide adoption.

This work proposes a target image search algorithm based on local features (TISLF) as outlined in Fig. 1. The process begins by downsampling the video stream and cutting it into segments that can be interpreted as corresponding to different camera angles or different scenes where objects can be assumed to move continuously throughout the scene. Within each segment, individual frames are analyzed and compared to each of the target images using a matching matrix obtained from SIFT descriptors. The most probable matches are then analyzed over time to remove spurious matches. Thus TISLF contains three stages: a video segmentation stage, a recognition stage, and an estimation stage. In principle, the matching method could be any algorithm based on local features; we demonstrate TISLF using the Scale-Invariant Feature Transform (SIFT) keypoints and RANSAC matches [7, 8, 13–15]. In the video segmentation stage, input video is cut into a sequence of segments based on a proposed matching

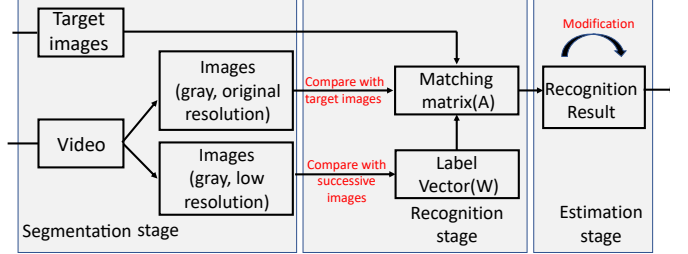


Fig. 1: Illustration of the TISLF. The algorithm consists of three stages: video segmentation, recognition, and estimation.

vector that represents the likelihood of change of scene. The recognition stage again uses SIFT (or other comparable local feature sets) to compute a matching matrix that can be interpreted as the probability that target images are contained within each of the images in the video segment. In the estimation stage, changes in the probabilities over time are used to reach final consensus on the presence (or absence) of the target images within each video segment.

The paper begins with a detailed description of the TISLF algorithm in Section II and then presents several experimental results that apply TISLF to different videos in Section III.

Our code is open source and can be found online at: <https://github.com/gbc8181/TISLF>.

II. TARGET IMAGE SEARCHING SYSTEM

The TISLF system consists of three stages which are described in full detail in sections II-A (segmentation), II-B (recognition), and II-C (estimation). In the first stage, the video is downsampled and cut into segments by computing a SIFT-based matching vector. In the recognition stage, each image in a segment is compared to the target images (using a SIFT-based matching matrix) resulting in a measure that can be interpreted as the raw probabilities that a given target is present in each image frame. The estimation stage then refines the raw probabilities by exploiting the continuity of the scene over time. TISLF operates efficiently to find sections of the video that contain the target images.

Suppose the video is sampled so that it contains m raw frames, each with dimension (H_r, W_r) . (For example, if a video were to be shot at 30 frames per second, a 30-times downsampling would provide an effective rate of 1 frame per second). Suppose also that there are N target images each with dimension (H_t, W_t) .

A. Segmentation Stage

The video segmentation stage transforms the source video to grayscale for higher computation speed, and maintains two

Bochen Guan and William Sethares are with the Department of Electrical and Computer Engineering, University of Wisconsin, Madison, WI, 53706 USA (e-mail: gbochen@wisc.edu). Hanrong Ye and Hong Liu are with Key Laboratory of Machine Perception, Shenzhen Graduate School, Peking University, China.

copies, X_1, X_2, \dots, X_m at the original resolution of (H_r, W_r) pixels and $\bar{X}_1, \bar{X}_2, \dots, \bar{X}_m$ downsampled to (\bar{H}_s, \bar{W}_s) pixels.

Temporal segmentation is carried out by calculating SIFT features and matches between consecutive pairs \bar{X}_i and \bar{X}_{i+1} . When successive images are similar to each other, they should have many matching keypoints; when a scene change or camera cut has occurred, the number of matching keypoints should be small. This measure of similarity can be formalized by counting the number of detected SIFT matching points divided by the total number of SIFT keypoints. Accordingly, let

$$p(\bar{X}_i, \bar{X}_{i+1}) = \frac{\# \text{ of matching points}}{\text{total } \# \text{ of keypoints}}. \quad (1)$$

Each element (1) lies between 0 and 1, and may be interpreted as the probability that two successive frames belong to the same video scene. These can be concatenated into the vector

$$W = (p(\bar{X}_1, \bar{X}_2), p(\bar{X}_2, \bar{X}_3), \dots, p(\bar{X}_{m-1}, \bar{X}_m)) \\ = (w_1, w_2, \dots, w_{m-1}) \quad (2)$$

which represents the successive similarities over time. Each element of W computes the match between neighboring frames.

The Page-Lorden CUSUM algorithm [16] can be applied to detect change points in the video using W . For example, if images $(\bar{X}_1, \bar{X}_2, \dots, \bar{X}_j)$ are shot from the same view but there is change of view starting from image \bar{X}_j onwards, the corresponding values $(w_1, w_2, \dots, w_{j-1})$ of W would be large, the similarity $w_j = p(\bar{X}_j, \bar{X}_{j+1})$ would be small, and the succeeding values w_k for $k > j$ would again be large. There are two hypotheses: $H_1 : w_1, w_2, \dots, w_j$ with mean value δ and $H_2 : w_{j+1}, \dots$ with mean value δ_2 . We know that δ is much larger than δ_2 and δ_2 is small enough. Assuming $\delta_2 = 0$, the stopping rule is

$$\inf\{\alpha : \max \delta \left(S_n - S_k - \delta \frac{(n-k)}{2} \right) \geq \alpha\} \quad (3)$$

where $S_n = \sum_{i=1}^n w_i$ is the cumulative sum of the w_i and α is a threshold specifying how much time must elapse before detecting the change point. The threshold can be determined from two parameters: ARL_0 and ARL_1 , which are used to estimate the performance of the algorithm [17].

This situation is depicted in Fig. 2(c), where G1 represents the initial scene, G2 represents the break between the scenes, and G3 is the final scene. For Page-Lorden CUSUM algorithm, G1 is H_1 and G2 is H_2 , we can detect the change point or breakdown between G1 and G2, so we believe that they are not in the same scenes. Analogously, G2 is H_2 and G3 is H_1 , we can also detect the change by Page-Lorden CUSUM algorithm, which segments the video into a collection of scenes. Subsequent processing is done on a per scene basis.

B. Recognition Stage

The recognition and estimation stages analyze each scene separately. Accordingly, suppose the image sequence (within a given scene) has $M \ll m$ images X_1, X_2, \dots, X_M (m is the number of frames). Each target image is partitioned into P vertical chunks S_k . The SIFT keypoints are used to establish a

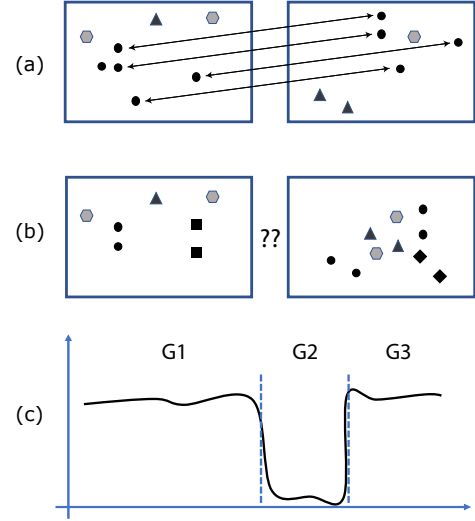


Fig. 2: Each shape represents a keypoint in the SIFT feature space for a successive pair of images \bar{X}_i and \bar{X}_{i+1} . (a) When there are many keypoints that are aligned (shown here by corresponding blocks of the same shade), $w_i = p(\bar{X}_i, \bar{X}_{i+1})$ is large and there is significant similarity between the two images. (b) When few keypoints align (shown by many blocks of disparate shading), $w_i = p(\bar{X}_i, \bar{X}_{i+1})$ is small and there is little similarity between the two images. (c) plots the sequence W . The Page-Lorden CUSUM algorithm is used to detect changes and to separate the images into different segments. G1 is the matching situation shown in (a), G2 is the no-matching situation shown in (b).

set of ground values by matching the targets with themselves. Since the targets are of size $L \times K$, TISLF divides every target image into P chunks of size $\frac{L \times K}{P}$. This self-matching process is shown in Fig. 3 and is calculated as

$$q(S_k) = \frac{\# \text{ matching points in chunk } k}{\# \text{ of keypoints in target image } k}. \quad (4)$$

Since each keypoint is also a matching point for the self-matching situation, we have

$$\sum_k q(S_k) = 1 \quad (5)$$

This provides M chunk distributions that can be used as a reference when matching the probability distributions of the target images.

The matching between the individual video images and the target images is again conducted using (4). So we can similarly use $p(S_k)$ to describe the keypoints matching between subsets of the target images (the chunks) and the video. Since not all keypoints can be matched,

$$p(S_k) = \frac{\# \text{ matching points in chunk } k}{\# \text{ of keypoints in target image } k}. \quad (6)$$

$$\sum_k p(S_k) \leq 1 \quad (7)$$

The image-target matching probability distribution can now be computed using the target-target self-matching distribution.

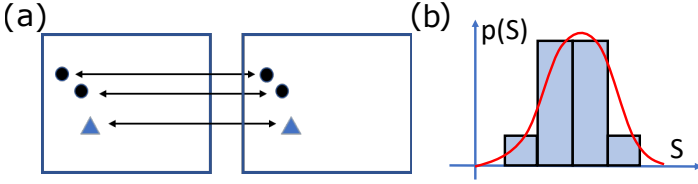


Fig. 3: Each shape represents a keypoint in the SIFT feature space for a target image and itself. (a) A sketch of target-target self-matching. (b) The number of matching keypoints between different target images defines the target-target matching probability distribution.

If the correlation of these two distributions is low, the target image T_j is unlikely to be in the image frame X_i . Here we can compute the Kullback–Leibler divergence of the two distributions to describe their correlations

$$D_{KL}(p||q) = \sum_k p(S_k) \log \frac{p(S_k)}{q(S_k)}. \quad (8)$$

A threshold α and the Kullback–Leibler divergence specify the correlated matching distributions, which are stored in a set R . This step is repeated for every video image and every target image.

In order to show the computation contains the complete information we use, we define a 3D matching matrix \mathbf{A} between video image X_i , target image T_j , and is calculated per chunk S_k . Thus \mathbf{A} has dimensions $M \times N \times P$ and each element is given by

$$\mathbf{A}_{i,j,k} = p(X_i, T_j, S_k) \text{ for } i \in (1, M), j \in (1, N), k \in (1, P).$$

Since the total matching points between a target image X_i and a video image T_j is the sum of the matching points in each chunk. Thus, the matching probability can be expressed as

$$\begin{aligned} p(X_i, T_j) &= \frac{\# \text{ matching points between } X_i \text{ and } T_j}{\text{total } \# \text{ of keypoints in } T_j} \\ &= \sum_{k \in (1, P)} p(X_i, T_j, S_k) \end{aligned} \quad (9)$$

and the 2D matching matrix A is simplified to

$$A = \begin{pmatrix} p(X_1, T_1) & p(X_1, T_2) & \dots & p(X_1, T_N) \\ p(X_2, T_1) & p(X_2, T_2) & \dots & p(X_2, T_N) \\ \dots & \dots & \dots & \dots \\ p(X_M, T_1) & p(X_M, T_2) & \dots & p(X_M, T_N) \end{pmatrix} \quad (10)$$

with dimensions $M \times N$.

By analyzing label vector W (2) from the segmentation stage, TISLF breaks matrix A into r subsets where each subset is in the same scene. To validate result of getting target images in video images, TISLF sorts matching probability of N targets in a subset $[p(X_i, T_1), p(X_i, T_2), \dots, p(X_i, T_M)]$. Then TISLF uses k-means clustering to pick highly distinctive matching probability set J . Comparing images in set R and J , if the image is found in both sets, the image is said to contain the target image.

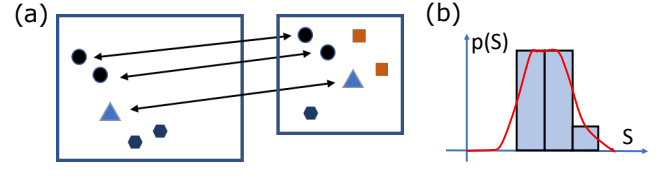


Fig. 4: Each shape represents a keypoint in the SIFT feature space for a video and a target image. (a) is a sketch of matching situation between a target and a video image. (b) We count the numbers of matching points between a target and a video image in different chunks of the target image. Thus, we obtain a matching probability distribution.

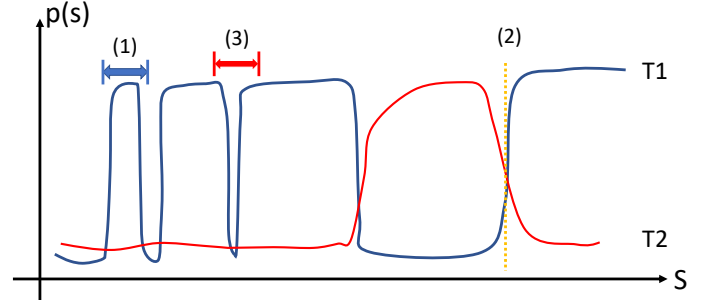


Fig. 5: A sketch of three conditions in estimation stage. (1) is the condition that time interval is less than t_{stand} (2) is the condition where GLRT applied (3) is the condition that time interval is less than t_{lost}

C. Estimation Stage

The Estimation Stage is applied to refine the estimates. A cross analysis of all video images in all scenes is used to determine which (if any) of the target images occur in each video scene. The output of the recognition stage is the raw distributions of matching probabilities between scene images X_1, X_2, \dots, X_M each target images T_j . Within a single continuous scene, it is expected that targets will generally persist for a significant number of frames; it is unreasonable for a target to appear, disappear, and re-appear in a short time. Thus the raw distributions may be smoothed by this assumed continuity over time. Assume that a sequence of video images X_i lie in the same scene G . Three parameters are developed to smooth the estimation of the probabilities within the scene: the minimum stand time t_{stand} , the maximum lost time t_{lost} and the generalized likelihood ratio test threshold β . These are illustrated in Fig.5.

1) *The Minimum Standing Time t_{stand}* : When a matching probability between a video image and a target image exceeds predefined threshold, it is a candidate match. If a target image is a candidate match only briefly (for a time less than t_{stand}), it is removed from consideration. On the other hand, if the target image persists (for a time greater than t_{stand}) it is accepted. See time interval (1) in Fig. 5 for an illustration.

2) *The Maximum Lost Time t_{lost}* : Suppose a candidate match T_j is present before time i , present after time $i + n$, but is absent for times in between. If this interval n is less than t_{lost} , then it is presumed that this absence is due to noise and so it is estimated to be present for the complete duration.

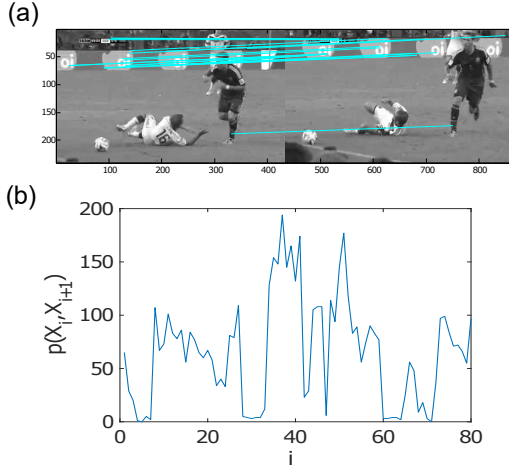


Fig. 6: (a) shows the matching points between two neighboring images. (b) shows the matching probabilities as a function of time. The images are divided into different segments when the matching probability decreases sharply.

Time interval (1) in Fig. 5. See time interval (3) in Fig. 5 for an illustration.

3) *Generalized Likelihood Ratio Test Threshold β* : Suppose that prior to time i , images X_i match target T_1 and after time $i + n$, images X_{i+n} match target T_2 . Then the decision of matches for times between i and $i + n$ can be made using a generalized likelihood ratio test (GLRT) [17, 18]. Let

$$\lambda(T) = \frac{\sup p(\bar{T}_1, \delta_{T1})}{\sup p(\bar{T}_2, \delta_{T2})} \quad (11)$$

where $\bar{T}_{1,(2)}$ is the mean value and $\delta_{T1(T2)}$ are the variances of the two target matching probabilities. By setting a threshold β to λ , assign these images to T_1 when $\lambda(T) > \beta$ and to T_2 when $\lambda(T) < \beta$. This is illustrated around location (2) in Fig. 5.

III. EXPERIMENTS

A. Advertising Board Search in Sports

Enterprises wish to know the commercial effectiveness of their advertisements in a sports game. One method is to count the total time that the advertising boards are seen over the duration of the game [19, 20]. Since games are commonly broadcast by the TV or over the Internet, it is possible to analyze the times of occurrence of the advertising boards over the duration of the game video.

TISLF provides a convenient method to solve this problem. To demonstrate, this section selects three different video clips from the 2014 FIFA World Cup [21]. In this soccer game, target images consist of a set of advertising boards paid for by Adidas, Coca Cola and Sony etc. The algorithm analyzes the video and reports on the (approximate) total duration that each advertisement is visible.

TISLF captures a large number of images from the video and compares each image with its neighbors using SIFT. Figure 6 illustrates the calculation of the matching probabilities between two successive images X_i and X_{i+1} . In Fig. 6(a),

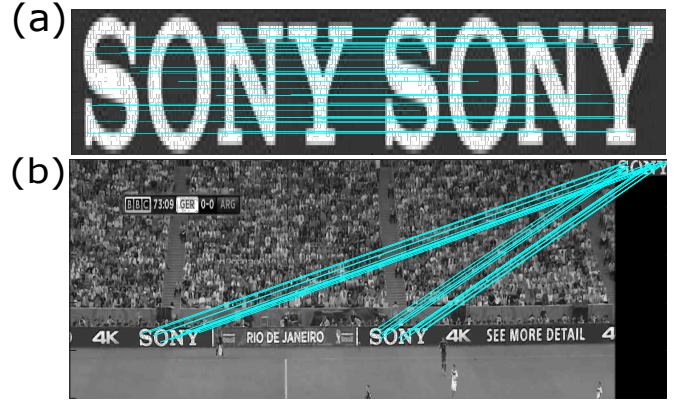


Fig. 7: (a) shows the matching of a target image with itself and (b) shows the matching between a target image and a video frame.

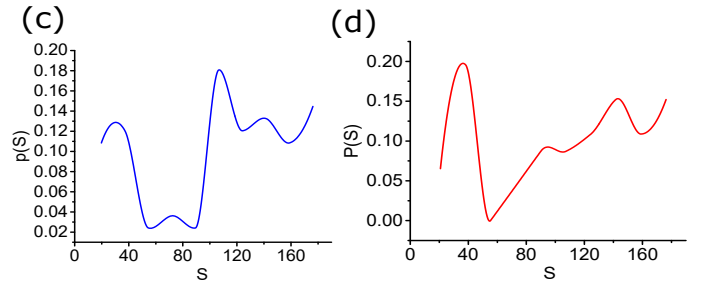


Fig. 8: Matching between the video images and target images. S is the horizontal position of the target image. (a) shows the matching probability distribution of target self matching which is used to normalize the calculation for this target. (b) shows the distribution of a target image T_j and a video image X_i .

the two frames are quite similar and so most of the SIFT keypoints match, thus giving a large value (i.e., close to 1). This is repeated for each successive pair and the probabilities are gathered as Fig. 6(b), which is then parsed using change point detection to segment the video and to assign labels to each segment.

Figure 7(a) illustrates the self matching between a target and itself (used for normalization of the matching probabilities) and (b) shows the matching keypoints between a target and a video image. These are used to calculate the matching probabilities and to compute their distribution. With target images self-matching probability distribution and target-video image matching probability distribution (shown in Fig. 8) and Fig. 9), TISLF conducts correlation tests and sets thresholds to estimate when the target-image distribution is similar to the reference. Fig.9 shows us a typical no-matching situation between the target image and the video frame.

TISLF next analyzes the matching probabilities between the video frames and the target images in the other two different dimensions (X_i and T_j). Based on these probability distributions, TISLF estimates the occurrence probability of each target image at every time and outputs a final result. TISLF is robust to situations when the video source images may be occluded. As shown in Fig. 10, TISLF can detect and recognize targets in video source images even though

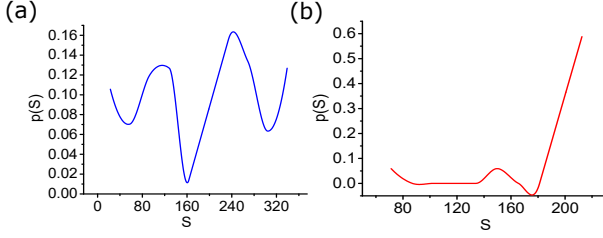


Fig. 9: No Matching situation between the a searching image and a target image. (a) shows the matching probability distribution of a target self matching. (b) shows the distribution of a target image T_j and a video image X_i . Since (b) and (a) have little similarity and correlation, the target image is not considered to exist in the video frame.



Fig. 10: shows a matching of a target image and video frame where the advertising board has been partly blocked.

some parts are blocked temporarily. Since TISLF is based on analysis about three different dimensions (X_i, T_j, S_k), part matching can show enough similarity between target images and video source images.

In order to verify the operation of the system, Fig. 11 shows the time of each target advertisement in the three football game videos compared to a ground truth which was determined by manually counting the number of frames each advertisement was visible. The average error ($= \frac{\text{computed time} - \text{ground truth time}}{\text{video time}}$) of TISLF is no more than 1 second/minute, which is well within the required accuracy [22].

B. Painting Search in a Documentary

Quite a number of documentaries about paintings and photographs are made each year. The producers may wish to know if there is a simple and fast way to index the paintings and/or photographs that appear in their film. Similarly, collectors may wish to track if and when their paintings are used. TISLF provides a definite answer to this problem. The experiments select a documentary [23] about Vincent van Gogh as the source video and attempts to determine the times of appearance of the paintings throughout the documentary.

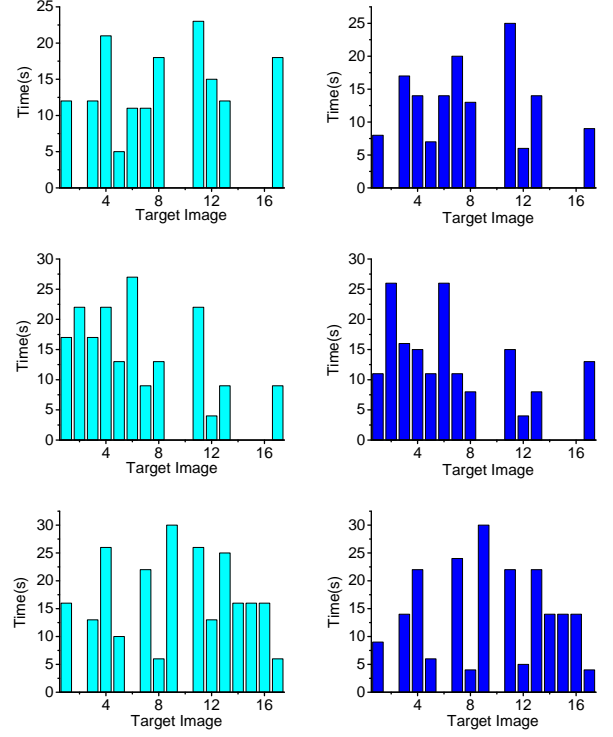


Fig. 11: The total time of each target image in present in three sports game videos. Horizontal coordinates represent different sequence number of target images/Ads and vertical coordinates represent the accounting time of each target. The light blue plots are the ground truth (determined by manually counting the time each target is present) and dark blue plots show the computed time using TISLF.

As demonstrated previously, TISLF groups the frames of the video into scenes; a vector W describes the segmentation result. The self-matching process is applied to the target paintings, giving the reference distribution $q(S_k)$. Then the target images and video images $p(S_k)$ are analyzed, and the highly correlated video images are recorded as set R . As shown in (10), images with a high matching probability are selected and stored in set J . The video images are in both R and J .

Since the images in one scene should be consistent, the appearance of target images should be uninterrupted. Two time spans are selected to record the matching results of pre and post images. Each matching result is analyzed and compared to ensure consistency. Fig. 12 shows the whole process of using TISLF to search for paintings in a documentary.

Results of the painting experiment are shown in Tab. I. As expected, the majority of the paintings are found and labeled correctly. Ground truth was established manually by carefully watching the videos and recording all views of the paintings.

Deep convolutional neural networks (CNNs) have been widely used in visual recognition tasks [24–26]. Among them, Residual networks (Resnet) [27, 28] are one of the most important neural networks commonly used for visual feature extraction. The next experiment compares the performance of Resnet in the image search tasks. The feature map just

TABLE I: Painting search in a documentary. The numbers represent the times that the painting appears in the video.

Painting No.	1	2	3	4	5	6	7	8	9	10	11	12
Times (Ground Truth)	1-9	20-23	37-39	0	55-60	75-81	84-85	86-91	92	102-108	117-119	0
Times (TISLF)	1-9	20-23	37-40	0	54-61	75-81	84-85	86-91	0	101-108	117-119	0
Times (Resnet-101)	1-9	20-23	37-39	40-41	55-60	17-19,75-81	84-85	7,16,68-91	92	10, 99-108	3, 117-199	0

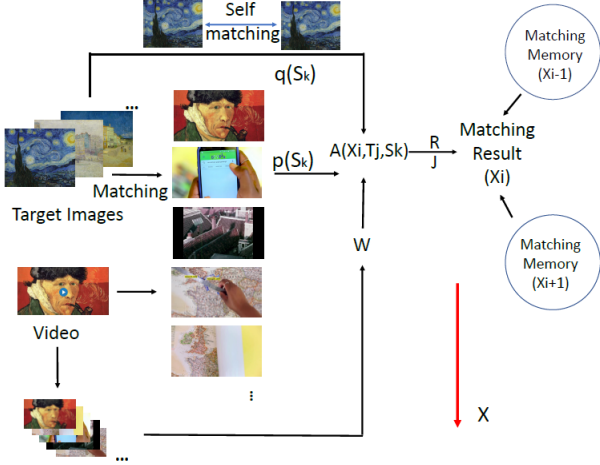


Fig. 12: Illustration of TISLF applied to painting search

prior to the the fully connected layer is extracted and the classification is conducted by calculating the cosine similarities [29] between pairs of feature maps. If the distance is above a threshold, the two images do not match. Since the retrieval performance is influenced by the threshold, we study the performance of the deep learning method using a variety of threshold values. The experiment adopts resnet-101 [27] which is pretrained on ImageNet [30] as the visual feature extractor. The final convolutional layer produces a feature map with dimension 2048.

To evaluate the performance of the image search, two metrics from information retrieval are adopted: Precision and Recall Rate [31], and both are evaluated on the Van Gogh documentary. Experimental results are shown in Table II. TISLF outperforms resnet at all threshold values. One possible explanation is that TISLF uses local features in the source image in order to uncover hidden features in contiguous frames. In contrast, the deep learning method uses global features extracted from the CNN applied to individual frames.

C. Landmark Search in Video

This experiment extends the model to pseudo-3D object detection in a video. We select several famous landmarks of different cities as target objects and a city documentary [32] as the source video. Since local feature algorithms are primarily applicable to 2D objects, we collect a set of images of each landmark taken from different viewing angles as the targets [33]. (Thus the target object is a series of images in place of a single image.) The goal is to locate these landmarks in the video. In an aerial view of a large city, several similar high architectures will influence the search process and increase the

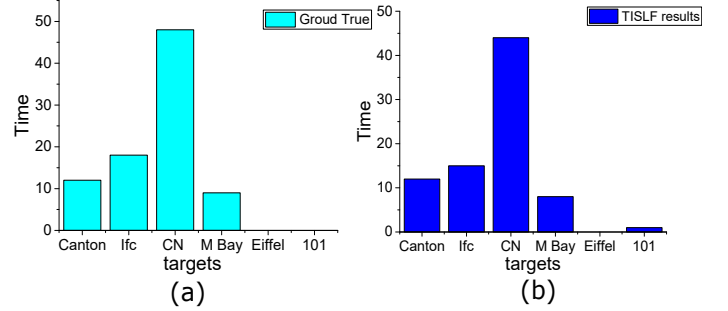


Fig. 13: The total time of each target landmarks in a documentary. The six landmarks are Canton tower, IFC Guangzhou, CN Tower, Mariana Bay, the Eiffel Tower, and Taipei 101.

probability of mismatch. Fig. 13 shows the results of searching for 6 city landmarks within the documentary. The accuracy of TISLF is quite acceptable.

IV. CONCLUSIONS

This paper introduced a target image search algorithm based on local features consisting of three stages: video segmentation, recognition, and estimation. An input video is cut into a series of segments based on their continuity. The matching probability matrix is combined with an estimation procedure to estimate the duration of the occurrences of each target image in the video. The system has been tested and verified in several experiments, and comparisons with state of the art deep learning methods suggest that the simpler TISLF can provide better performance while requiring less computational effort.

V. ACKNOWLEDGEMENT

Bochen Guan is supported by Oversea Study scholarship of Guangzhou Elite. Hanrong Ye and Hong Liu are supported by National Natural Science Foundation of China (NSFC, U1613209), specialized Research Fund for Strategic and Prospective Industrial Development of Shenzhen City (No. ZLZBCXLJZI20160729 020003).

REFERENCES

- [1] Fei Yu, Chao Li, Qiang Mei, and Zhe Lin, "A novel method of wide searching scope and fast searching speed for image block matching," in *Applied Optics and Photonics China (AOPC2015)*. International Society for Optics and Photonics, 2015, pp. 96780F–96780F.
- [2] H. T. Nguyen, M. Worring, and A. Dev, "Detection of moving objects in video using a robust motion similarity measure," *IEEE Transactions on Image Processing*, vol. 9, no. 1, pp. 137–141, Jan 2000.

TABLE II: Painting search in a documentary of Van Gogh with Resnet-101 [27]. The feature map before the last linear layer is extracted for calculating similarity distance. T is the threshold used in the cosine similarity. TISLF outperforms even the optimized neural network.

Method	Precision	Recall Rate
ResNet101 (T=0.90)	1.00	0.18
ResNet101 (T=0.85)	1.00	0.46
ResNet101 (T=0.80)	0.73	0.58
ResNet101 (T=0.75)	0.41	0.75
ResNet101 (T=0.70)	0.21	0.89
TISLF	0.92	0.94

- [3] S. C. Wong, V. Stamatescu, A. Gatt, D. Kearney, I. Lee, and M. D. McDonnell, "Track everything: Limiting prior knowledge in online multi-object recognition," *IEEE Transactions on Image Processing*, vol. 26, no. 10, pp. 4669–4683, Oct 2017.
- [4] W. Wang, J. Shen, and L. Shao, "Video salient object detection via fully convolutional networks," *IEEE Transactions on Image Processing*, vol. 27, no. 1, pp. 38–49, Jan 2018.
- [5] Wu Liu, Tao Mei, Yongdong Zhang, Cherry Che, and Jiebo Luo, "Multi-task deep visual-semantic embedding for video thumbnail selection," in *Proceedings of the IEEE Conference on Computer Vision and Pattern Recognition*, 2015, pp. 3707–3715.
- [6] Masoud Mazloom, Efstratios Gavves, Koen van de Sande, and Cees Snoek, "Searching informative concept banks for video event detection," in *Proceedings of the 3rd ACM conference on International conference on multimedia retrieval*. ACM, 2013, pp. 255–262.
- [7] Sebastiano Battiato, Giovanni Gallo, Giovanni Puglisi, and Salvatore Scellato, "Sift features tracking for video stabilization," in *Image Analysis and Processing, 2007. ICIAP 2007. 14th International Conference on*. IEEE, 2007, pp. 825–830.
- [8] Xuelong Hu, Yingcheng Tang, and Zhenghua Zhang, "Video object matching based on sift algorithm," in *Neural Networks and Signal Processing, 2008 International Conference on*. IEEE, 2008, pp. 412–415.
- [9] Shuangbao Paul Wang, Carolyn Maher, Xiaolong Cheng, and William Kelly, "Invideo: An automatic video index and search engine for large video collections," *SIGNAL 2017 Editors*, p. 34, 2017.
- [10] Ken Chatfield, Relja Arandjelović, Omkar Parkhi, and Andrew Zisserman, "On-the-fly learning for visual search of large-scale image and video datasets," *International journal of multimedia information retrieval*, vol. 4, no. 2, pp. 75, 2015.
- [11] Y. Zhang, X. Chen, J. Li, W. Teng, and H. Song, "Exploring weakly labeled images for video object segmentation with submodular proposal selection," *IEEE Transactions on Image Processing*, vol. 27, no. 9, pp. 4245–4259, Sept 2018.
- [12] H. Fu, D. Xu, and S. Lin, "Object-based multiple foreground segmentation in rgb-d video," *IEEE Transactions on Image Processing*, vol. 26, no. 3, pp. 1418–1427, March 2017.
- [13] Luo Juan and Oubong Gwun, "A comparison of sift, pca-sift and surf," *International Journal of Image Processing (IJIP)*, vol. 3, no. 4, pp. 143–152, 2009.
- [14] Konstantinos G Derpanis, "Overview of the ransac algorithm," *Image Rochester NY*, vol. 4, no. 1, pp. 2–3, 2010.
- [15] Rahul Raguram, Jan-Michael Frahm, and Marc Pollefeys, "A comparative analysis of ransac techniques leading to adaptive real-time random sample consensus," *Computer Vision–ECCV 2008*, pp. 500–513, 2008.
- [16] Douglas M Hawkins and Qifan Wu, "The cusum and the ewma head-to-head," *Quality Engineering*, vol. 26, no. 2, pp. 215–222, 2014.
- [17] David Siegmund and ES Venkatraman, "Using the generalized likelihood ratio statistic for sequential detection of a change-point," *The Annals of Statistics*, pp. 255–271, 1995.
- [18] Jianqing Fan, Chunming Zhang, and Jian Zhang, "Generalized likelihood ratio statistics and wilks phenomenon," *Annals of statistics*, pp. 153–193, 2001.
- [19] Peng Chang, Mei Han, and Yihong Gong, "Extract highlights from baseball game video with hidden markov models," in *Image Processing. 2002. Proceedings. 2002 International Conference on*. IEEE, 2002, vol. 1, pp. I–I.
- [20] John L Sherry, Kristen Lucas, Bradley S Greenberg, and Ken Lachlan, "Video game uses and gratifications as predictors of use and game preference," *Playing video games: Motives, responses, and consequences*, vol. 24, pp. 213–224, 2006.
- [21] "Holland vs argentina 2014 semi-final full match 1 - youtube," YouTube video, July 10 2014, Accessed Aug. 1, 2018.
- [22] Federico Perazzi, Jordi Pont-Tuset, Brian McWilliams, Luc Van Gool, Markus Gross, and Alexander Sorkine-Hornung, "A benchmark dataset and evaluation methodology for video object segmentation," in *Proceedings of the IEEE Conference on Computer Vision and Pattern Recognition*, 2016, pp. 724–732.
- [23] Vox, "Vincent van gogh's long, miserable road to fame," YouTube video, Jul. 15 2017, Accessed Aug. 1, 2018.
- [24] Y. Yang, Z. Zhong, Shen T., and Z. Lin, "Convolutional neural networks with alternately updated cliques," in *Proceedings of the IEEE Conference on Computer Vision and Pattern Recognition*, 2018, pp. 4700–4709.
- [25] G. Huang, L. Zhuang, L. Maaten, and K. Weinberger, "Densely connected convolutional networks," in *Pro-*

- ceedings of the IEEE Conference on Computer Vision and Pattern Recognition*, 2017, pp. 4700–4709.
- [26] R Girshick, J. Donahue, T. Darrell, and J. Malik, “Rich feature hierarchies for accurate object detection and semantic segmentation,” in *Proceedings of the IEEE Conference on Computer Vision and Pattern Recognition*, 2014, pp. 580–587.
 - [27] K. He, X. Zhang, S. Ren, and J. Sun, “Deep residual learning for image recognition,” in *Proceedings of the IEEE Conference on Computer Vision and Pattern Recognition*, 2016, pp. 770–778.
 - [28] Liang-Chieh Chen, George Papandreou, Iasonas Kokkinos, Kevin Murphy, and Alan L Yuille, “Deeplab: Semantic image segmentation with deep convolutional nets, atrous convolution, and fully connected crfs,” *IEEE transactions on pattern analysis and machine intelligence*, vol. 40, no. 4, pp. 834–848, 2018.
 - [29] Chengjun Liu and Harry Wechsler, “Gabor feature based classification using the enhanced fisher linear discriminant model for face recognition,” *IEEE Transactions on Image processing*, vol. 11, no. 4, pp. 467–476, 2002.
 - [30] Olga Russakovsky, Jia Deng, Hao Su, Jonathan Krause, Sanjeev Satheesh, Sean Ma, Zhiheng Huang, Andrej Karpathy, Aditya Khosla, Michael Bernstein, Alexander C. Berg, and Li Fei-Fei, “ImageNet Large Scale Visual Recognition Challenge,” *International Journal of Computer Vision (IJCV)*, vol. 115, no. 3, pp. 211–252, 2015.
 - [31] W. B. Farakes and R. Baeza-Yates, *Information Retrieval: Data Structures and Algorithms*, vol. 331, Englewood Cliffs, NJ: prentice Hall, 3 edition, 7 1992.
 - [32] “Top 10 skylines in the world 2017,” YouTube video, Dec. 25 2017, Accessed Jun. 2, 2018.
 - [33] Shengshan Hu, Qian Wang, Jingjun Wang, Zhan Qin, and Kui Ren, “Securing sift: Privacy-preserving outsourcing computation of feature extractions over encrypted image data,” *IEEE Transactions on Image Processing*, vol. 25, no. 7, pp. 3411–3425, 2016.